Available online at www.sciencedirect.com
SCIENCE DIRECT®
PERGAMON
International Journal of Heat and Mass Transfer 46 (2003) 3167–3178
International Journal of HEAT and MASS TRANSFER
www.elsevier.com/locate/ijhmt

The Brinkman model for the mixed convection boundary layer flow past a horizontal circular cylinder in a porous medium

Roslinda Nazar [a], Norsarahaida Amin [a], Diana Filip [b], Ioan Pop [b,*]

[a] Department of Mathematics, Universiti Teknologi Malaysia, 81310 Johor Bahru, Johor, Malaysia
[b] Department of Applied Mathematics, Faculty of Mathematics, University of Cluj, R-3400 Cluj, CP 253, Romania

Received 10 February 2003

Abstract

The Brinkman model is used for the theoretical study of the mixed convection boundary layer flow past a horizontal circular cylinder with a constant surface temperature and embedded in a fluid-saturated porous medium in a stream flowing vertically upwards. Both the cases of a heated (assisting flow) and a cooled (opposing flow) cylinder are considered. It is shown that there are two governing dimensionless parameters, which are related to thermal and viscous effects. These are the Darcy–Brinkman parameter Γ and the mixed convection parameter λ. It is shown that for $\Gamma = 0$ the problem reduces to the similarity Darcy's model, while for $\Gamma \neq 0$ the governing equations are non-similar and they have been solved numerically using the Keller-box method. It is found that heating the cylinder ($\lambda > 0$) delays separation of the boundary layer and can, if the cylinder is warm enough (large values of $\lambda > 0$), suppress it completely. On the other hand, cooling the cylinder ($\lambda < 0$) brings the boundary layer separation point nearer to the lower stagnation point and for sufficiently cold cylinder (large values of $\lambda < 0$) there will not be a boundary layer on the cylinder. A complete physical description of the problem is presented throughout the analysis. Some results were given in the form of tables. Such tables are very important and they can serve as a reference against which other exact or approximate solutions can be compared in the future.

1. Introduction

Convective heat transfer in porous media has been a subject of great interest for the last several decades. This interest was motivated by numerous thermal engineering applications in various disciplines, such as geophysical thermal and insulation engineering, the modelling of packed sphere beds, the cooling of electronic systems, groundwater hydrology, chemical catalytic reactors, ceramic processes, grain storage devices, fiber and granular insulation, petroleum reservoirs, coal combustors, ground water pollution and filtration processes, to name just a few of these applications. Much of the recent work on this topic is reviewed by Nield and Bejan [1], Ingham and Pop [2], Vafai [3], and Pop and Ingham [4]. In most previous studies, either on free or combined convection in porous media, boundary layer treatments based on Darcy's law and Forschheimer—extended Darcy's law models have been considered. However, it is well known that Darcy's law is an empirical formula relating the pressure gradient, the bulk viscous resistance and the gravitational force in a porous medium. Thus, the formulation of convective heat transfer problems based on Darcy's law completely neglects the viscous force acting along the impermeable surface. Fand et al. [5] carried out an experimental investigation of free convection from a horizontal circular cylinder embedded in a porous medium, and reported that deviations from the Darcy's law occur when the Reynolds number based on the pore diameter exceeds 1–10. Thus, the non-Darcy

* Corresponding author.
E-mail address: popi@math.ubbcluj.ro (I. Pop).

0017-9310/03/$ - see front matter
doi:10.1016/S0017-9310(03)00122-4

Nomenclature

a	radius of the cylinder
C_f	skin friction coefficient
Da	Darcy number based on a
f	reduced stream function
g	gravitational acceleration
K	permeability of the porous medium
Nu	Nusselt number
p	pressure
Pe	Péclet number
Pr	Prandtl number
Ra	Rayleigh number for a porous medium
T	fluid temperature
u	dimensionless velocity in the x-direction
$u_e(x)$	dimensionless free stream velocity
v	dimensionless velocity in the y-direction
x, y	dimensionless Cartesian coordinates along the surface of the cylinder and normal to it, respectively

Greek symbols

α_m	effective thermal diffusivity of porous medium
β	thermal expansion coefficient
δ_{i1}, δ_{i2}	delta Kronecker operators
Γ	Darcy–Brinkman parameter
ϕ	porosity
η	transformed variable
λ	mixed convection parameter
μ	dynamic viscosity of the fluid
ν	kinematic viscosity of the fluid
θ	dimensionless fluid temperature
ρ	density
ψ	dimensionless stream function

Superscripts

–	dimensional quantities
$'$	differentiation with respect to y or η

Subscripts

w	condition at the wall
∞	ambient condition

flow situation is more likely to prevail when the Rayleigh number is sufficiently high that the boundary layer approximations are relevant.

For flow through a porous medium with a high permeability, Brinkman [6] as well as Chan et al. [7], argue that the momentum equation for a porous medium flow must reduce to the viscous flow limit and advocate that classical frictional terms be added in Darcy's law. The Brinkman model with the addition of the convective terms and under the boundary layer approximation was used by Evans and Plumb [8] for a numerical study of free convection about an isothermal vertical flat plate embedded in a porous medium. Their numerical results show that the value of the local Nusselt number is in agreement with the Cheng–Minkowycz theory [9] (based on the Darcy's law) if the Darcy number based on the length of the plate is less than 10^{-7}. For higher values of the Darcy number, they found that their numerical results for the local Nusselt number are slightly smaller than those given by the Cheng–Minkowycz theory [9] for the free convection boundary layer along a vertical flat plate embedded in a porous medium. Vafai and Tien [10] used the Brinkman model to study the problem of forced convection over an impermeable heated plate embedded in a porous medium. They defined a momentum boundary layer as the layer adjacent to the surface where the viscous effect on the surface and the bulk viscous force are equally important. The existence of the momentum boundary layer near the heated surface was shown to retard the streamwise velocity close to the wall, resulting in a decrease of the surface heat flux. The effect is found to be most pronounced near the leading edge of the plate and in a fluid with a high Prandtl number. The Brinkman model was also used by Hsu and Cheng [11], Kim and Vafai [12], and Hong et al. [13] to study the boundary effects in a free convection porous layer adjacent to a semi-infinite vertical flat plate with a power law variation of wall temperature, i.e. x^m, where x measures the distance along the plate and m is a constant. It was shown that the non-dimensional governing equations contain two small parameters ε and σ, where $\varepsilon = (Ra)^{-1/2}$ and $\sigma = (Da/\phi)^{1/2}$, with Ra and Da being the Rayleigh number and the Darcy number, respectively, and ϕ is the porosity of the porous medium. For the limit of $\varepsilon \to 0$, $\sigma \to 0$ and $\sigma \ll \varepsilon$, a perturbation solution for the problem is obtained using the method of matched asymptotic expansions. It is shown that the physical problem consists of three layers: the inner viscous sub-layer with a thickness of $O(\sigma)$, which has been called by Vafai and Tien [10], as the momentum boundary layer; the middle thermal layer with a thickness of $O(\varepsilon)$; and the outer potential region with a thickness of $O(1)$. Chen et al. [14] studied the problem of mixed convection boundary layer flow about a vertical cylinder embedded in a porous medium by taking the non-Darcian effects into consideration, while Hossain et al. [15] studied the non-Darcy forced convection boundary layer flow over a wedge embedded in a

porous medium and discussed the effects of the convective inertia term, Forschheimer term (or porous inertia term), and the Brinkman term (or boundary friction term) on the skin friction and the rate of heat transfer.

In this paper, we use the transformations proposed by Merkin [16] for the mixed convection boundary layer flow past a horizontal circular cylinder immersed in a viscous (non-porous) and incompressible fluid to study the problem of mixed convection boundary layer flow past a horizontal circular cylinder embedded in a porous medium using the Brinkman model. It is shown that the solution depends on the non-dimensional Darcy–Brinkman parameter Γ and the mixed convection parameter λ with $\lambda > 0$ for a heated cylinder ($T_w > T_\infty$) and $\lambda < 0$ for a cooled cylinder ($T_w < T_\infty$), respectively. The case $\lambda = 0$ is the forced convection solution. The parameter Γ represents the effect of viscous layer on the thermal layer, while λ represents the effect of forced to free convection. For small values of $|\lambda|$ forced convection effects dominate, while for large values of $|\lambda|$ it is the free convection which is important, so that values of λ of $O(1)$, where both effects are comparable, are of most interest. Letting $\Gamma = 0$ is equivalent to neglecting the viscous layer effect and the problem reduces to that of mixed convection boundary layer flow about a horizontal cylinder embedded in a Darcian porous medium, which is first studied by Cheng [17] using a similarity transformation. For $\Gamma \neq 0$ we have solved numerically the transformed non-similar boundary layer equations using the Keller-box method [18]. This method has been very successfully recently used by the present authors [19–21] for solving some analogous problems for viscous fluids and also for micropolar fluids. Both the cases $\lambda > 0$ (assisting flow) and $\lambda < 0$ (opposing flow) are discussed in the present paper. We found that for $\Gamma \neq 0$ and $\lambda > 0$ both the forced and free convection boundary layers start at the lower (bottom) stagnation point of the cylinder with the buoyancy forces accelerating the fluid in the boundary layer. There is a value of $\lambda = \lambda_s(\Gamma)$ (say) for which the boundary layer starts to separate. For $\lambda > \lambda_s(\Gamma)$, the boundary layer remains on the cylinder and starts to separate just before the upper (top) stagnation point ($x = \pi$) to form a plume. This situation is different from that found by Merkin [16], where the boundary layer remains on the cylinder up to the upper stagnation point ($x = \pi$). For $\Gamma \neq 0$ and $\lambda < 0$, on the other hand, the buoyancy forces also retard the fluid and so the separation point is brought nearer to the lower stagnation point. A value of $\lambda = \lambda_0(\Gamma)$ (say) is found for which the boundary layer separates at this point and it is shown that for values of λ less than $\lambda_0(\Gamma)$ a boundary layer solution is not possible. However, the actual value of $\lambda_s(\Gamma)$ which first gives no separation is difficult to determine exactly, while the value of $\lambda_0(\Gamma)$ can be exactly determined. Further, we have shown that for very small value of Γ, or Darcy flow model, the present results are in very good agreement with those obtained by solving the similarity equations found by Cheng [17]. Thus, the results are believed to be very consistent which, potentially, make them of importance to future theoretical studies of convective flow problems in porous media. To our best knowledge the present problem has not been considered before and we believe that the results reported here are important for some geophysical and engineering applications.

2. Basic equations

Consider the problem of steady mixed convection flow past a horizontal circular cylinder of radius a embedded in a fluid-saturated porous medium as shown in Fig. 1, where $\bar{x}$ is the coordinate in the streamwise direction along the surface of the cylinder measured from the lower stagnation point, and $\bar{y}$ is the coordinate normal to the surface. It is assumed that the surface of the cylinder is held at a constant temperature T_w, while the ambient temperature is T_∞. It is also assumed that a free stream $(1/2)u_\infty$ is flowing vertically upwards over the cylinder so that the free stream velocity for the boundary layer is $\bar{u}_e(\bar{x}) = u_\infty \sin(\bar{x}/a)$. Under the Boussinesq approximation, the governing equations with inertia and thermal dispersion effects neglected are (see [1])

$$\frac{\partial \bar{u}}{\partial \bar{x}} + \frac{\partial \bar{v}}{\partial \bar{y}} = 0 \tag{1}$$

$$\frac{\mu}{K}\bar{u} = \frac{\mu}{\phi}\left(\frac{\partial^2 \bar{u}}{\partial \bar{x}^2} + \frac{\partial^2 \bar{u}}{\partial \bar{y}^2}\right) - \frac{\partial p}{\partial \bar{x}} - \rho g \sin(\bar{x}/a) \tag{2}$$

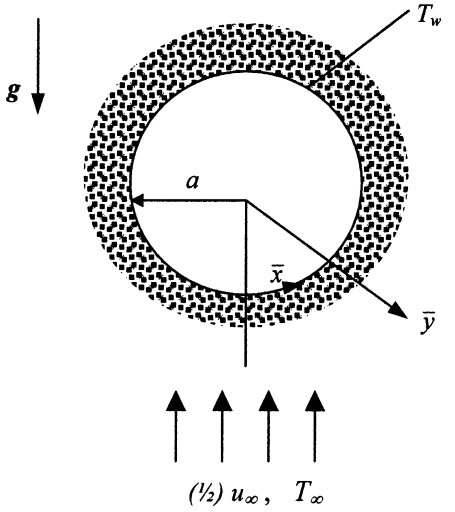

Fig. 1. Physical model and coordinate system.

$$\frac{\mu}{K}\bar{v}=\frac{\mu}{\phi}\left(\frac{\partial^2\bar{v}}{\partial\bar{x}^2}+\frac{\partial^2\bar{v}}{\partial\bar{y}^2}\right)-\frac{\partial p}{\partial\bar{y}}+\rho g\cos(\bar{x}/a) \tag{3}$$

$$\rho=\rho_\infty[1-\beta(T-T_\infty)] \tag{4}$$

$$\bar{u}\frac{\partial T}{\partial\bar{x}}+\bar{v}\frac{\partial T}{\partial\bar{y}}=\alpha_{\mathrm{m}}\left(\frac{\partial^2 T}{\partial\bar{x}^2}+\frac{\partial^2 T}{\partial\bar{y}^2}\right) \tag{5}$$

subject to the boundary conditions

$$\begin{aligned}&\bar{u}=\bar{v}=0,\quad T=T_{\mathrm{w}}\quad\text{on}\quad\bar{y}=0\\&\bar{u}\to\bar{u}_{\mathrm{e}}(\bar{x}),\quad T\to T_\infty\quad\text{as}\quad\bar{y}\to\infty\end{aligned} \tag{6}$$

where $\bar{u}$ and $\bar{v}$ are the velocity components along $\bar{x}$- and $\bar{y}$-axes, respectively, T is the fluid temperature, p is the pressure, K is the permeability of the porous medium, g is the acceleration due to gravity, α_{m} is the effective thermal diffusivity of the porous medium, β is the thermal expansion coefficient, ρ is the density, μ is the dynamic viscosity of the fluid and ϕ is the porosity of the porous medium.

We introduce now the boundary layer variables

$$\begin{aligned}&x=\bar{x}/a,\quad y=Pe^{1/2}(\bar{y}/a),\quad u=\bar{u}/u_\infty,\quad v=Pe^{1/2}(\bar{v}/u_\infty),\\&\theta=(T-T_\infty)/(T_{\mathrm{w}}-T)_\infty,\quad u_{\mathrm{e}}(x)=\bar{u}_{\mathrm{e}}(\bar{x})/u_\infty\end{aligned} \tag{7}$$

where $Pe=u_\infty a/\alpha_{\mathrm{m}}$ is the modified Péclet number for a porous medium.

If we eliminate the pressure p from Eqs. (2) and (3), and assume that $Pe\to\infty$ (boundary layer approximation), Eqs. (1)–(5) can be reduced to the following dimensionless form

$$\frac{\partial u}{\partial x}+\frac{\partial v}{\partial y}=0 \tag{8}$$

$$\frac{\partial u}{\partial y}=\Gamma\frac{\partial^3 u}{\partial y^3}+\lambda\frac{\partial\theta}{\partial y}\sin x \tag{9}$$

$$u\frac{\partial\theta}{\partial x}+v\frac{\partial\theta}{\partial y}=\frac{\partial^2\theta}{\partial y^2} \tag{10}$$

while the boundary conditions (6) become

$$\begin{aligned}&u=v=0,\quad\theta=1\quad\text{on}\quad y=0\\&u\to u_{\mathrm{e}}(x),\quad\theta\to0\quad\text{as}\quad y\to\infty\end{aligned} \tag{11}$$

where the Darcy–Brinkman parameter Γ and the mixed convection parameter λ are given by

$$\Gamma=\frac{Da}{\phi}Pe,\quad\lambda=\frac{Ra}{Pe} \tag{12}$$

with Da and Ra being the Darcy and the Rayleigh numbers, respectively, which are defined as

$$Da=\frac{K}{a^2},\quad Ra=\frac{gK\beta(T_{\mathrm{w}}-T_\infty)a}{\alpha_{\mathrm{m}}\nu} \tag{13}$$

Further, if we integrate once Eq. (9) subject to the boundary conditions (11) and introduce the stream function ψ defined as

$$u=\frac{\partial\psi}{\partial y},\quad v=-\frac{\partial\psi}{\partial x} \tag{14}$$

Eqs. (9) and (10) can then be written as

$$\frac{\partial\psi}{\partial y}-u_{\mathrm{e}}(x)=\Gamma\frac{\partial^3\psi}{\partial y^3}+\lambda\theta\sin x \tag{15}$$

$$\frac{\partial\psi}{\partial y}\frac{\partial\theta}{\partial x}-\frac{\partial\psi}{\partial x}\frac{\partial\theta}{\partial y}=\frac{\partial^2\theta}{\partial y^2} \tag{16}$$

and the boundary conditions (11) become

$$\begin{aligned}&\psi=\frac{\partial\psi}{\partial y}=0,\quad\theta=1\text{ on }y=0\\&\frac{\partial\psi}{\partial y}\to u_{\mathrm{e}}(x),\quad\theta\to0\text{ as }y\to\infty\end{aligned} \tag{17}$$

where $u_{\mathrm{e}}(x)=\sin x$. We notice that for $\Gamma=0$ (Darcy's model), Eqs. (15)–(17) can be reduced to the similarity equations found by Cheng [17] (except a factor of 1/2, which can be scaled out from these equations) and they can be written as

$$f'=1+\lambda\theta \tag{18}$$

$$\theta''+f\theta'=0$$

subject to the boundary conditions

$$\begin{aligned}&f(0)=0,\quad\theta(0)=1\\&f'(\infty)=1,\quad\theta(\infty)=0\end{aligned} \tag{19}$$

or

$$f'''+ff''=0 \tag{20}$$

subject to the boundary conditions

$$f(0)=0,\quad f'(0)=1+\lambda,\quad f'(\infty)=1 \tag{21}$$

where primes denote differentiation with respect to y.

We look now for a solution of Eqs. (15) and (16) of the form proposed by Merkin [16]

$$\psi=xf(x,y),\quad\theta=\theta(x,y) \tag{22}$$

Then, we have to solve the following equations

$$\Gamma\frac{\partial^3 f}{\partial y^3}+\frac{\partial f}{\partial y}=(1+\lambda\theta)\frac{\sin x}{x} \tag{23}$$

$$\frac{\partial^2\theta}{\partial y^2}+f\frac{\partial\theta}{\partial y}=x\left(\frac{\partial f}{\partial y}\frac{\partial\theta}{\partial x}-\frac{\partial f}{\partial x}\frac{\partial\theta}{\partial y}\right) \tag{24}$$

along with the boundary conditions

$$\begin{aligned}&f=\frac{\partial f}{\partial y}=0,\quad\theta=1\text{ on }y=0\\&\frac{\partial f}{\partial y}\to\frac{\sin x}{x},\quad\theta\to0\text{ as }y\to\infty\end{aligned} \tag{25}$$

The physical quantities of interest in this problem are the skin friction coefficient C_f and the Nusselt number Nu, which can be expressed as

$$(Pe^{1/2}/Pr)C_f = x\frac{\partial^2 f}{\partial y^2}(x,0), \quad Nu/Pe^{1/2} = -\frac{\partial \theta}{\partial y}(x,0) \tag{26}$$

where $Pr = \upsilon/\alpha_m$ is the Prandtl number for the porous medium.

At the lower stagnation point of the cylinder, $x \cong 0$, Eqs. (23) and (24) reduce to the following ordinary differential equations

$$\Gamma f''' - f' + 1 + \lambda\theta = 0 \tag{27}$$

$$\theta'' + f\theta' = 0 \tag{28}$$

subject to

$$\begin{aligned} &f(0) = f'(0) = 0, \quad \theta(0) = 1 \\ &f' \to 1, \quad \theta \to 0 \text{ as } y \to \infty \end{aligned} \tag{29}$$

For $\Gamma \neq 0$, $\lambda > 0$ and $\lambda \gg 1$, we introduce the following transformation

$$f = \lambda^{1/4}F(\eta), \quad \theta = G(\eta), \quad \eta = \lambda^{1/4}y \tag{30}$$

Eqs. (27) and (28) then become

$$\Gamma F''' + G - F'\lambda^{-1/2} + \lambda^{-1} = 0 \tag{31}$$

$$G'' + FG' = 0 \tag{32}$$

subject to

$$\begin{aligned} &F(0) = F'(0) = 0, \quad G(0) = 1 \\ &F' \to \lambda^{-1/2}, \quad G \to 0 \text{ as } \eta \to \infty \end{aligned} \tag{33}$$

We look now for a solution of Eqs. (31) and (32) of the form

$$\begin{aligned} F &= F_0(\eta) + F_1(\eta)\lambda^{-1/2} + F_2(\eta)\lambda^{-1} + \text{h.o.t.} \\ G &= G_0(\eta) + G_1(\eta)\lambda^{-1/2} + G_2(\eta)\lambda^{-1} + \text{h.o.t.} \end{aligned} \tag{34}$$

for $\lambda \gg 1$, where the functions F_0 and G_0 are given by the equations

$$\Gamma F_0''' + G_0 = 0 \tag{35}$$

$$G_0'' + F_0G_0' = 0 \tag{36}$$

subject to

$$\begin{aligned} &F_0(0) = F_0'(0) = 0, \quad G_0(0) = 1 \\ &F_0' \to 0, \quad G_0 \to 0 \text{ as } \eta \to \infty \end{aligned} \tag{37}$$

We notice that these equations describe the free convection near the lower stagnation point of a circular cylinder embedded in a fluid-saturated porous medium based on the Brinkman model ($\Gamma \neq 0$). Further, the functions F_i and G_i ($i \geqslant 1$) are given by the equations

$$\Gamma F_i''' - F_{i-1}' + G_i + \delta_{i2} = 0 \tag{38}$$

$$G_i'' + \sum_{j=0}^{i} F_{i-j}G_i' = 0 \tag{39}$$

subject to

$$\begin{aligned} &F_i(0) = F_i'(0) = 0, \quad G_i(0) = 0 \\ &F_i' \to \delta_{i1}, \quad G_i \to 0 \text{ as } \eta \to \infty \end{aligned} \tag{40}$$

where δ_{i1} and δ_{i2} are the delta Kronecker operators. Therefore, we have

$$\begin{aligned} f''(0) &= \lambda^{3/4}[F_0''(0) + F_1''(0)\lambda^{-1/2} + F_2''(0)\lambda^{-1} + \text{h.o.t}] \\ \theta'(0) &= \lambda^{3/4}[G_0'(0) + G_1'(0)\lambda^{-1/2} + G_2'(0)\lambda^{-1} + \text{h.o.t}] \end{aligned} \tag{41}$$

for $\lambda \gg 1$.

3. Results and discussion

The transformed non-similar boundary layer Eqs. (23) and (24) subject to the boundary conditions (25) are solved numerically for different values of the parameters Γ and λ, and at some streamwise positions x using the Keller-box method as described by Cebeci and Bradshaw [18]. The ordinary differential equations (18)–(21) for the Darcy's flow model ($\Gamma = 0$) as well as Eqs. (27)–(29) and (35)–(40), valid at the lower stagnation point of the cylinder ($x \cong 0$), are also solved numerically using the Keller-box method. In order to check our solution, we have calculated the heat transfer from the cylinder, $-\theta'(0)$, by solving Eqs. (18) and (19) for some values of the parameter λ in the range $-1 \leqslant \lambda \leqslant 20$ and compared these results with those reported by Cheng [22] (with a factor of 1/2). Some values of $-\theta'(0)$ are given in Table 1 and we can see that the agreement between these solutions is excellent. Further, it is worth mentioning that in

Table 1
Values of $-\theta'(0)$ for $\Gamma = 0$ (Darcy model) and various values of λ

λ	Ref. [22]	Present (Keller-box)
−1.0	0.3320	0.3321
−0.8	0.3916	0.3917
−0.6	0.4420	0.4421
−0.4	0.4865	0.4866
−0.2	0.5269	0.5270
0.0	0.5641	0.5642
0.5	0.6473	0.6474
1.0	0.7205	0.7206
3.0	0.9574	0.9576
10.0	1.516	1.5167
20.0	2.066	2.067

Table 2
Values of $f''(0)$ for different values of $\lambda(<0)$

λ	Ref. [23]		Present (Keller-box)	
	$f_1''(0)$	$f_2''(0)$	$f_1''(0)$	$f_2''(0)$
−1.00	0.46960		0.46960	
−1.05	0.46758	0.00004	0.46759	0.00001
−1.10	0.46105	0.00194	0.46106	0.00190
−1.15	0.44907	0.00866	0.44909	0.00866
−1.20	0.43015	0.02219	0.43017	0.02218
−1.25	0.40152	0.04539	0.40156	0.04538
−1.30	0.35664	0.08497	0.35684	0.08487
−1.35	0.25758	0.17856	0.26240	0.17851
−1.354	0.22428		0.23274	

the assisting case ($\lambda > 0$), solutions of Eqs. (18) and (19) are possible for all values of λ. However, for opposing flow ($\lambda < 0$), Merkin [23] was the first to show that a solution of Eqs. (20) and (21) is possible only for a limited range values of λ, namely $-1.354 \leqslant \lambda \leqslant 0$. For $-1.354 < \lambda < -1$ the solution is non-unique and two values of the reduced skin friction coefficient, $f''(0)$ exist for a given value of λ as can be seen from Table 2. It is seen again from this table that our results are in very good agreement with those found by Merkin [23].

Further, we have calculated in Table 3 values of the reduced skin friction coefficient, $f''(0)$, and wall heat transfer, $-\theta'(0)$, for some values of the parameter Γ when $\Gamma = 0$ (Darcy model) and when $\Gamma \neq 0$ (Brinkman model), respectively, by solving Eqs. (27)–(29) valid at the lower stagnation point ($x \cong 0$). Only small values of $\Gamma(\ll 1)$ were considered as it is the case that usually exists in geophysical and engineering applications (see [11]). The results obtained by Cheng [22] for the Darcy flow model ($\Gamma = 0$) were also included in this table. It can be seen from this table that for the Darcy flow model ($\Gamma = 0$) the results are again in excellent agreement. This table shows further that for large values of the mixed convection parameter $\lambda(\gg 1)$ the numerical and series solutions given by (41), are also in a good agreement. Therefore, we are confident that the present results are accurate enough.

Some values of the skin friction coefficient, $(Pe^{1/2}/Pr)C_f$, and the Nusselt number, $Nu/Pe^{1/2}$, are given in Tables 4–7 and presented in Figs. 2–8 for some values of Γ, λ and x. These tables and figures show that the boundary layer separates from the cylinder for some values of $\lambda < 0$ (opposing flow). Increasing λ delays separation and the separation can be completely suppressed in the range $0 \leqslant x < \pi$ for sufficiently large values of λ. A value of $\lambda = \lambda_0(\Gamma)(< 0)$ is found below which the boundary layer solution is not possible. However, there is a value of $\lambda = \lambda_s(\Gamma)(< 0)$ for which the boundary layer starts to separate. It is seen further from Tables 4–7 and Figs. 2–8 that the value of $\lambda_s(\Gamma)$ which first gives no separation lies between −1.03 and −1.02 for $\Gamma = 0.1$, and between −1.06 and −1.05 for $\Gamma = 0.3$. For $\lambda > \lambda_s(\Gamma)$, the boundary layer remains on the cylinder and starts to separate just before the upper (top) stagnation point ($x = \pi$) to form a plume where values of the skin friction and the heat transfer become negative, as can be seen from Tables 4–7 and Figs. 2–8. This situation is different from that found by Merkin [16] for the corresponding problem in a viscous (non-porous medium) fluid, where the boundary layer remains on the cylinder up to the upper stagnation point.

Further, we mention that we have obtained also the velocity and temperature profiles for some values of the Darcy–Brinkman and mixed convection parameters Γ and λ, respectively, at different x positions around the cylinder but for the sake of saving space we will not present these profiles here. Thus, it was found that the velocity profiles and the skin friction decrease with the increase of Γ as can be seen from Fig. 7. However, the temperature profiles increase with increasing Γ. Thus, the thermal boundary layer thickness is increased, the temperature gradient at the wall is decreased and the heat transfer rate is reduced as can be seen from Fig. 8. This is because when Γ becomes larger, the Darcy resistance due to the presence of the solid matrix is dominant, and the effect of the no-slip condition is restricted in a viscous layer. When the thickness of this viscous layer is much smaller than the thickness of the thermal boundary layer, the no-slip condition can be neglected and Darcy's model can be employed [13].

Finally, Figs. 9 and 10 show the variation of the separation point with $\lambda(< 0)$ for $\Gamma = 0.1$ and 0.3. The actual value of $\lambda_s(\Gamma)(< 0)$ which first gives no separation is difficult to determine exactly as it has to be found by successive integrations of the equations. These figures also show that there is a value of $\lambda = \lambda_0(\Gamma)(< 0)$ below which a boundary layer solution is not possible. It is also seen from these figures that the value of $\lambda_s(\Gamma)(< 0)$ and $\lambda_0(\Gamma)(< 0)$ increases with increasing the value of Γ.

Table 3
Values of $f''(0)$ and $-\theta'(0)$ at the lower stagnation point of the cylinder ($x \cong 0$) for $\Gamma = 0$, 0.1, 0.2 and 0.3, and various values of λ

λ	Darcy model [22]	$\Gamma = 0$ (present)	$\Gamma = 0.1$				$\Gamma = 0.2$				$\Gamma = 0.3$			
	Numerical (Keller-box)	Numerical Eqs. (27) and (28) (Keller-box)	Numerical Eqs. (27) and (28)		Series Eq. (41)		Numerical Eqs. (27) and (28)		Series Eq. (41)		Numerical Eqs. (27) and (28)		Series Eq. (41)	
	$-\theta'(0)$	$-\theta'(0)$	$f''(0)$	$-\theta'(0)$	$f''(0)$	$-\theta'(0)$	$f''(0)$	$-\theta'(0)$	$f''(0)$	$-\theta'(0)$	$f''(0)$	$-\theta'(0)$	$f''(0)$	$-\theta'(0)$
−1.27											−0.0132	0.3878		
−1.26											0.0046	0.3909		
−1.25											0.0223	0.3940		
−1.22							−0.0133	0.3987			0.0746	0.4028		
−1.21							0.0087	0.4020			0.0918	0.4056		
−1.20							0.0305	0.4052			0.1089	0.4083		
−1.16			−0.0299	0.4130			0.1168	0.4176			0.1764	0.4189		
−1.15			0.0016	0.4166			0.1380	0.4206			0.1930	0.4215		
−1.1	0.4192	0.4193	0.1569	0.4339			0.2429	0.4347			0.2750	0.4337		
−1.0	0.4697	0.4698	0.4588	0.4647			0.4460	0.4600			0.4339	0.4558		
−0.5	0.6575	0.6576	1.8619	0.5781			1.3806	0.5549			1.1624	0.5396		
0.0	0.7980	0.7980	3.1623	0.6976			2.2361	0.6652			1.8257	0.6426		
0.5	0.9157	0.9156	4.3999	0.7240			3.0437	0.6784			2.4497	0.6500		
1.0	1.0192	1.0191	5.5923	0.7791			3.8173	0.7251			3.0457	0.6919		
2.0	1.1988	1.1987	7.8768	0.8706			5.2901	0.8026			4.1768	0.7616		
3.0	1.3543	1.3541	10.0613	0.9460	10.3375	1.1864	6.6897	0.8663	6.8509	1.0308	5.2485	0.8190	5.4772	0.9353
4.0	1.4934	1.4932	12.1697	1.0107	12.3970	1.2167	8.0344	0.9210	8.2004	1.0796	6.2759	0.8683	6.4021	0.9792
5.0	1.6204	1.6202	14.2167	1.0678	14.4434	1.2469	9.3354	0.9693	9.4522	1.1022	7.2681	0.9117	7.4052	1.0071
6.0	1.7382	1.7380	16.2124	1.1191	16.3674	1.2799	10.6002	1.0126	10.7176	1.1448	8.2313	0.9508	8.3410	1.0355
7.0	1.8484	1.8481	18.1642	1.1658	18.2118	1.3034	11.8341	1.0521	11.8494	1.1763	9.1699	0.9864	9.2765	1.0632
8.0	1.9523	1.9520	20.0774	1.2089	20.0728	1.3362	13.0413	1.0885	13.0001	1.2063	10.0872	1.0192	10.0553	1.0897
9.0	2.0510	2.0505	21.9566	1.2489	21.9478	1.3604	14.2248	1.1222	14.1090	1.2349	10.9858	1.0496	10.9050	1.1150
10.0	2.1451	2.1444	23.8051	1.2863	23.7343	1.3948	15.3871	1.1538	15.2356	1.2521	11.8676	1.0780	11.6663	1.1391
20.0	2.9243	2.9223	41.0660	1.5720	40.4810	1.6771	26.1781	1.3945	25.2752	1.4769	20.0297	1.2951	19.3719	1.3307

Table 4
Values of the skin friction coefficient $(Pe^{1/2}/Pr)C_f$ for $\Gamma = 0.1$ and various values of λ

x	λ										
	−1.13	−1.10	−1.03	−1.02	−1.0	−0.5	0.0	1.0	2.0	5.0	10.0
0.0	0.0000	0.0000	0.0000	0.0000	0.0000	0.0000	0.0000	0.0000	0.0000	0.0000	0.0000
0.2	0.0121	0.0306	0.0727	0.0787	0.0905	0.3691	0.6274	1.1101	1.5639	2.8236	4.7290
0.4	0.0207	0.0569	0.1397	0.1513	0.1745	0.7212	1.2281	2.1759	3.0673	5.5424	9.2879
0.6		0.0754	0.1958	0.2127	0.2464	1.0411	1.7782	3.1573	4.4552	8.0614	13.5223
0.8		0.0836	0.2371	0.2587	0.3017	1.3151	2.2558	4.0175	5.6768	10.2913	17.2863
1.0		0.0800	0.2609	0.2864	0.3371	1.5318	2.6419	4.7234	6.6862	12.1514	20.4469
1.2		0.0645	0.2661	0.2945	0.3510	1.6823	2.9212	5.2477	7.4446	13.5716	22.8875
1.4		0.0388	0.2534	0.2836	0.3437	1.7610	3.0825	5.5691	7.9214	14.4946	24.5108
1.6		0.0058	0.2250	0.2558	0.3171	1.7657	3.1196	5.6736	8.0948	14.8777	25.2415
1.8			0.1846	0.2149	0.2750	1.6973	3.0310	5.5545	7.9532	14.6939	25.0278
2.0			0.1375	0.1658	0.2223	1.5605	2.8204	5.2132	7.4953	13.9324	23.8426
2.2			0.0891	0.1145	0.1648	1.3627	2.4962	4.6590	6.7300	12.5991	21.6831
2.4			0.0456	0.0668	0.1088	1.1141	2.0716	3.9087	5.6765	10.7161	18.5695
2.6			0.0126	0.0285	0.0603	0.8270	1.5634	2.9862	4.3637	8.3202	14.5410
2.8			0.0038	0.0058	0.0253	0.5152	0.9922	1.9217	2.8288	5.4599	9.6478
3.0				0.0011	0.0080	0.1935	0.3807	0.7499	1.1143	2.1865	3.9261
π				−0.0002	−0.0013	−0.0311	−0.0621	−0.1240	−0.1858	−0.3706	−0.6747

Table 5
Values of the local Nusselt number $Nu/Pe^{1/2}$ for $\Gamma = 0.1$ and various values of λ

x	λ										
	−1.13	−1.10	−1.03	−1.02	−1.0	−0.5	0.0	1.0	2.0	5.0	10.0
0.0	0.4237	0.4339	0.4559	0.4589	0.4647	0.5781	0.6976	0.7791	0.8706	1.0678	1.2863
0.2	0.4210	0.4312	0.4532	0.4562	0.4620	0.5752	0.6734	0.7758	0.8671	1.0638	1.2818
0.4	0.4138	0.4241	0.4461	0.4491	0.4549	0.5676	0.6505	0.7670	0.8577	1.0531	1.2697
0.6		0.4125	0.4345	0.4374	0.4432	0.5552	0.6360	0.7527	0.8428	1.0357	1.2500
0.8		0.3966	0.4185	0.4215	0.4237	0.5383	0.6174	0.7328	0.8212	1.0115	1.2226
1.0		0.3765	0.3984	0.4013	0.4071	0.5167	0.5941	0.7074	0.7940	0.9805	1.1874
1.2		0.3524	0.3742	0.3771	0.3828	0.4905	0.5660	0.6765	0.7608	0.9426	1.1443
1.4		0.3245	0.3462	0.3491	0.3547	0.4597	0.5331	0.6399	0.7215	0.8975	1.0930
1.6		0.2932	0.3147	0.3175	0.3230	0.4246	0.4953	0.5976	0.6759	0.8451	1.0331
1.8			0.2799	0.2826	0.2879	0.3851	0.4526	0.5495	0.6239	0.7849	0.9640
2.0			0.2421	0.2448	0.2499	0.3415	0.4050	0.4953	0.5651	0.7163	0.8851
2.2			0.2019	0.2044	0.2092	0.2936	0.3524	0.4347	0.4989	0.6385	0.7949
2.4			0.1598	0.1621	0.1664	0.2416	0.2943	0.3670	0.4244	0.5499	0.6914
2.6			0.1169	0.1187	0.1222	0.1851	0.2302	0.2909	0.3399	0.4478	0.5708
2.8			0.0803	0.0801	0.0807	0.1235	0.1585	0.2040	0.2419	0.3268	0.4251
3.0				0.0712	0.0660	0.0544	0.0747	0.0986	0.1204	0.1706	0.2309
π				0.0709	0.0658	−0.0020	−0.0102	−0.0110	−0.0128	−0.0162	−0.0183

4. Conclusions

Mixed convection boundary layer flow from a horizontal circular cylinder embedded in a fluid-saturated porous medium using the Brinkman model has been analyzed in detail. The numerical solutions of the governing equations have been obtained using the Keller-box method and the results are presented over the range of physically relevant buoyancy parameter values $\lambda > \lambda_0(\Gamma)$, which model the case in which the buoyancy forces are both assisting and opposing the free stream. We have sought to determine how the mixed convection parameter λ and the Darcy–Brinkman parameter Γ affect the flow and heat transfer characteristics as well as the position of the boundary layer separation point x_s. From this study we can draw the following conclusions:

- the flow and heat transfer characteristics predicted by considering the Brinkman model differ significantly from those based on Darcy's law. In this case the velocity in the boundary layer is reduced, resulting in a lower heat transfer rate;

Table 6
Values of the skin friction coefficient $(Pe^{1/2}/Pr)C_f$ for $\Gamma = 0.3$ and various values of λ

x	λ												
	−1.25	−1.20	−1.15	−1.10	−1.06	−1.05	−1.0	−0.5	0.0	1.0	2.0	5.0	10.0
0.0	0.0000	0.0000	0.0000	0.0000	0.0000	0.0000	0.0000	0.0000	0.0000	0.0000	0.0000	0.0000	0.0000
0.2	0.0039	0.0211	0.0378	0.0541	0.0669	0.0701	0.0857	0.2304	0.3622	0.6047	0.8294	1.4438	2.3594
0.4	0.0046	0.0385	0.0714	0.1035	0.1286	0.1348	0.1656	0.4500	0.7091	1.1856	1.6275	2.8356	4.6366
0.6		0.0490	0.0971	0.1439	0.1806	0.1897	0.2346	0.6492	1.0267	1.7213	2.3657	4.1282	6.7569
0.8		0.0502	0.1120	0.1722	0.2192	0.2309	0.2884	0.8193	1.3025	2.1919	3.0175	5.2770	8.6495
1.0		0.0407	0.1145	0.1860	0.2419	0.2557	0.3239	0.9530	1.5254	2.5797	3.5591	6.2416	10.2497
1.2			0.1039	0.1844	0.2473	0.2628	0.3394	1.0448	1.6866	2.8698	3.9700	6.9867	11.5001
1.4			0.0812	0.1681	0.2357	0.2524	0.3347	1.0912	1.7798	3.0507	4.2339	7.4828	12.3523
1.6			0.0490	0.1392	0.2091	0.2264	0.3113	1.0910	1.8012	3.1143	4.3387	7.7075	12.7676
1.8				0.1014	0.1709	0.1880	0.2723	1.0451	1.7501	3.0567	4.2776	7.6452	12.7182
2.0				0.0597	0.1259	0.1422	0.2223	0.9566	1.6286	2.8777	4.0485	7.2881	12.1866
2.2				0.0206	0.0801	0.0948	0.1670	0.8309	1.4414	2.5816	3.6542	6.6352	11.1658
2.4					0.0401	0.0523	0.1127	0.6750	1.1963	2.1759	3.1023	5.6920	9.6570
2.6					0.0125	0.0213	0.0660	0.4972	0.9030	1.6720	2.4046	4.4689	7.6666
2.8					0.0007	0.0058	0.0321	0.3069	0.5732	1.0841	1.5756	2.9776	5.1976
3.0						0.0012	0.0106	0.1142	0.2202	0.4277	0.6306	1.2209	2.2249
π						0.0004	−0.0011	−0.0177	−0.0354	−0.0710	−0.1064	−0.2120	−0.2720

Table 7
Values of the local Nusselt number $Nu/Pe^{1/2}$ for $\Gamma = 0.3$ and various values of λ

x	λ												
	−1.25	−1.20	−1.15	−1.10	−1.06	−1.05	−1.0	−0.5	0.0	1.0	2.0	5.0	10.0
0.0	0.3943	0.4086	0.4217	0.4339	0.4430	0.4452	0.4559	0.5397	0.5257	0.6919	0.7616	0.9117	1.0795
0.2	0.3916	0.4060	0.4191	0.4313	0.4405	0.4427	0.4534	0.5372	0.5936	0.6892	0.7588	0.9086	1.0760
0.4	0.3843	0.3989	0.4122	0.4245	0.4338	0.4360	0.4467	0.5305	0.5905	0.6820	0.7512	0.9002	1.0667
0.6		0.3875	0.4011	0.4135	0.4228	0.4251	0.4359	0.5197	0.5798	0.6702	0.7388	0.8865	1.0515
0.8		0.3718	0.3857	0.3983	0.4078	0.4100	0.4209	0.5048	0.5646	0.6539	0.7217	0.8675	1.0303
1.0		0.3517	0.3661	0.3791	0.3886	0.3909	0.4020	0.4858	0.5450	0.6330	0.6997	0.8430	1.0032
1.2			0.3425	0.3558	0.3656	0.3679	0.3791	0.4626	0.5212	0.6075	0.6728	0.8131	0.9698
1.4			0.3149	0.3287	0.3387	0.3411	0.3524	0.4354	0.4931	0.5773	0.6410	0.7774	0.9301
1.6			0.2836	0.2980	0.3082	0.3106	0.3220	0.4042	0.4608	0.5422	0.6039	0.7359	0.8838
1.8				0.2640	0.2744	0.2768	0.2883	0.3690	0.4241	0.5022	0.5615	0.6881	0.8302
2.0				0.2273	0.2378	0.2402	0.2516	0.3299	0.3829	0.4569	0.5133	0.6334	0.7688
2.2				0.1891	0.1991	0.2015	0.2124	0.2867	0.3370	0.4059	0.4586	0.5710	0.6984
2.4					0.1604	0.1624	0.1719	0.2394	0.2859	0.3482	0.3964	0.4992	0.6170
2.6					0.1259	0.1268	0.1324	0.1875	0.2287	0.2824	0.3246	0.4153	0.5211
2.8					0.1037	0.1028	0.1002	0.1303	0.1633	0.2051	0.2393	0.3132	0.4033
3.0						0.0923	0.0834	0.0655	0.0840	0.1067	0.1278	0.1747	0.2410
π						0.0888	0.0784	0.0144	−0.0022	−0.0077	−0.0098	−0.0128	0.0302

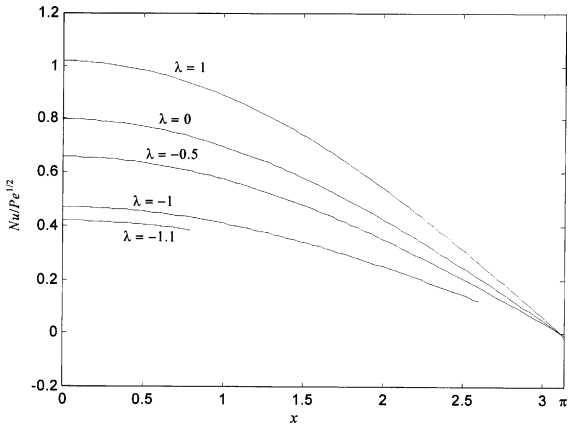

Fig. 2. Variation of the local Nusselt number with x for $\Gamma = 0$ and various values of λ.

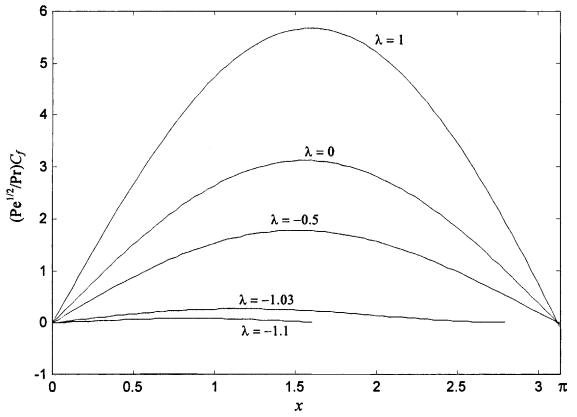

Fig. 3. Variation of the skin friction coefficient with x for $\Gamma = 0.1$ and various values of λ.

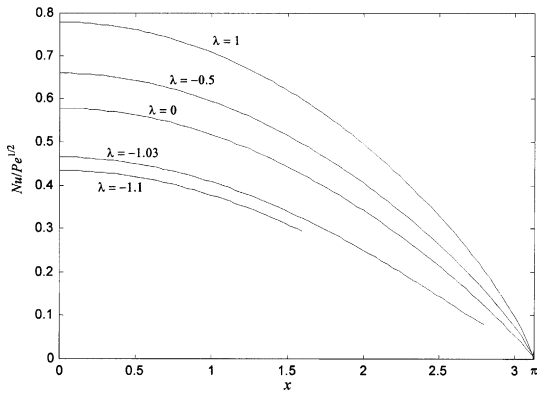

Fig. 4. Variation of the local Nusselt number with x for $\Gamma = 0.1$ and various values of λ.

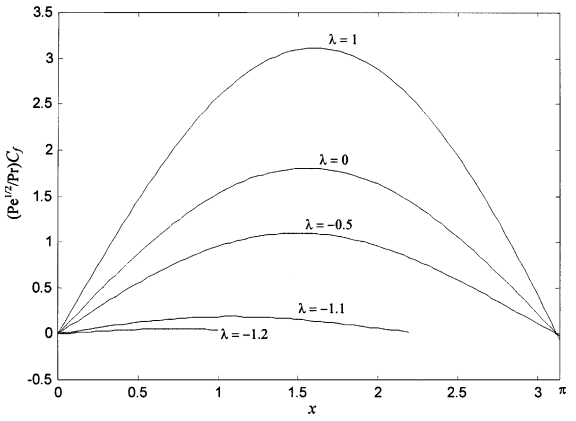

Fig. 5. Variation of the skin friction coefficient with x for $\Gamma = 0.3$ and various values of λ.

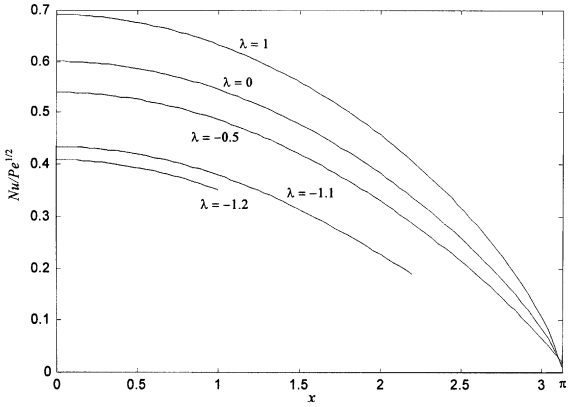

Fig. 6. Variation of the local Nusselt number with x for $\Gamma = 0.3$ and various values of λ.

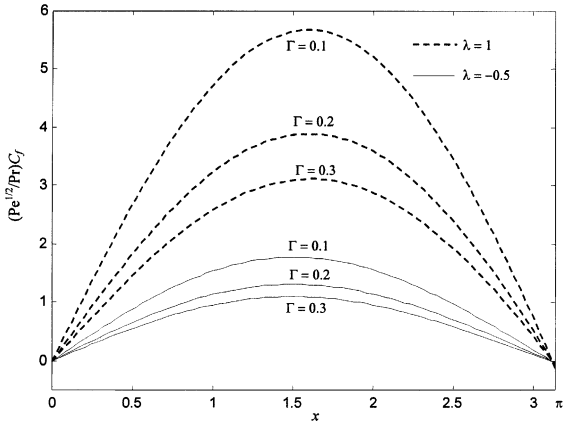

Fig. 7. Variation of the skin friction coefficient with x for $\Gamma = 0.1$, 0.2, 0.3 and $\lambda = 1$, -0.5.

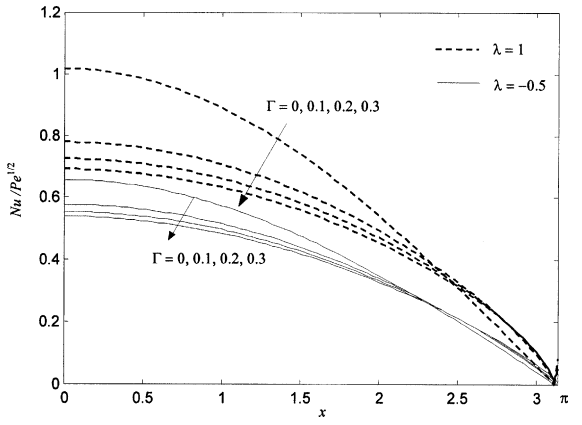

Fig. 8. Variation of the local Nusselt number with x for $\Gamma = 0$, 0.1, 0.2, 0.3, $\lambda = 1, -0.5$.

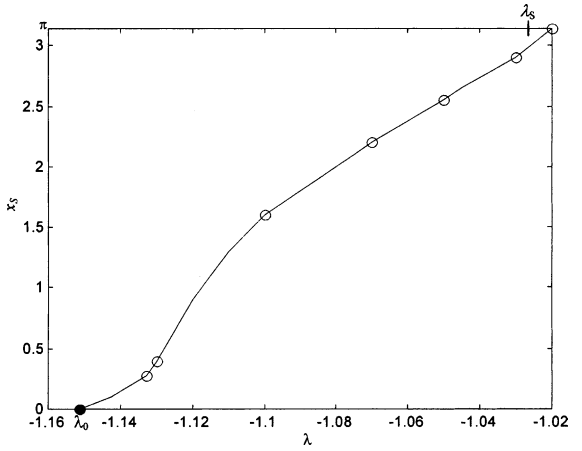

Fig. 9. Variation of separation point x_s for $\Gamma = 0.1$ with various λ.

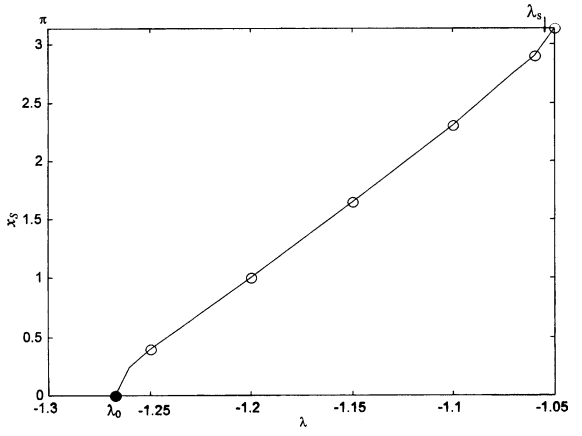

Fig. 10. Variation of separation point x_s for $\Gamma = 0.3$ with various λ.

- an increase in the value of Γ leads to a decrease of the wall heat transfer and the skin friction coefficient;
- an increase in the value of Γ leads to an increase of the value of $\lambda = \lambda_s(\Gamma)(< 0)$ which first gives no separation. The increase of Γ also leads to an increase of $\lambda_0(\Gamma)(< 0)$ below which a boundary layer solution is not possible.

Acknowledgements

The authors wish to thank the Ibn Sino Institute for Fundamental Science Studies of Universiti Teknologi Malaysia for financial support and for giving one of the authors (IP) the chance to visit this University.

References

[1] D.A. Nield, A. Bejan, Convection in Porous Media, second ed., Springer, New York, 1999.
[2] D.B. Ingham, I. Pop (Eds.), Transport Phenomena in Porous Media, Pergamon, Oxford, 1998, vol. II, 2002.
[3] K. Vafai (Ed.), Handbook of Porous Media, Marcel Dekker, Marcel, 2000.
[4] I. Pop, D.B. Ingham, Convective Heat Transfer: mathematical and computational modelling of viscous fluids and porous media, Pergamon, Oxford, 2001.
[5] R.M. Fand, T.E. Steinberg, P. Cheng, Natural convection heat transfer from a horizontal cylinder embedded in a porous medium, Int. J. Heat Mass Transfer 29 (1986) 119–133.
[6] H.C. Brinkman, A calculation of the viscous force exerted by a flowing fluid on a dense swarm of particles, Appl. Sci. Res. 1 (1947) 27–34.
[7] B.K.C. Chan, C.M. Iney, I.M. Barry, Natural convection in enclosed porous media with rectangular boundaries, J. Heat Transfer 92 (1970) 21–27.
[8] G.H. Evans, O.A. Plumb, Natural convection from a vertical isothermal surface embedded in a saturated porous medium, in: Proceedings of the AIAA-ASME Thermophysics and Heat Transfer Conference, Paper No. 78-HT-55, 1978.
[9] P. Cheng, W.J. Minkowycz, Free convection about a vertical flat plate embedded in a porous medium with applications to heat transfer from a dike, J. Geophys. Res. 82 (1977) 2040–2044.
[10] K. Vafai, C.L. Tien, Boundary and inertia effects on flow and heat transfer in porous media, Int. J. Heat Mass Transfer 24 (1981) 195–203.
[11] C.T. Hsu, P. Cheng, The Brinkman model for the natural convection about a semi-infinite vertical flat plate in a porous medium, Int. J. Heat Mass Transfer 28 (1985) 683–697.
[12] S.J. Kim, K. Vafai, Analysis of natural convection about a vertical plate embedded in a porous medium, Int. J. Heat Mass Transfer 32 (1989) 665–677.
[13] J.T. Hong, C.L. Tien, M. Kaviany, Non-Darcian effects on vertical-plate natural convection in porous media with high porosities, Int. J. Heat Mass Transfer 28 (1985) 2149–2157.

[14] C.-K. Chen, C.-H. Chen, W.J. Minkowycz, U.S. Gill, Non-Darcian effects on mixed convection about a vertical cylinder embedded in a saturated porous medium, Int. J. Heat Mass Transfer 35 (1992) 3041–3046.
[15] M.A. Hossain, N. Banu, A. Nakayama, Non-Darcy forced convection boundary layer flow over a wedge embedded in a saturated porous medium, Numer. Heat Transfer, Part A 26 (1994) 399–414.
[16] J.H. Merkin, Mixed convection from a horizontal circular cylinder, Int. J. Heat Mass Transfer 20 (1977) 73–77.
[17] P. Cheng, Mixed convection about a horizontal cylinder and a sphere in a fluid-saturated porous medium, Int. J. Heat Mass Transfer 25 (1982) 1245–1247.
[18] T. Cebeci, P. Bradshaw, Physical and Computational Aspects of Convective Heat Transfer, Springer, New York, 1984.
[19] R. Nazar, N. Amin, I. Pop, Mixed convection boundary layer flow from a horizontal circular cylinder in micropolar fluids: case of constant wall temperature, Int. J. Numer. Meth. Heat Fluid Flow 13 (2003) 86–109.
[20] R. Nazar, N. Amin, I. Pop, Mixed convection boundary layer flow from a horizontal circular cylinder with a constant surface heat flux, Heat Mass Transfer, in press.
[21] R. Nazar, N. Amin, I. Pop, On the mixed convection boundary layer flow about a solid sphere with constant surface temperature, Arab. J. Sci. Eng. 27 (2002) 1–19.
[22] P. Cheng, Combined free and forced convection flow about inclined surfaces in porous media, Int. J. Heat Mass Transfer 20 (1977) 807–814.
[23] J.H. Merkin, Mixed convection boundary layer flow on a vertical surface in a saturated porous medium, J. Eng. Math. 14 (1980) 301–313.